

Imaging, Anatomical, and Molecular Analysis of Callosal Formation in the Developing Human Fetal Brain

TIANBO REN,¹ AURORA ANDERSON,² WEI-BIN SHEN,¹ HAO HUANG,³
CELINE PLACHEZ,¹ JIANGYANG ZHANG,³ SUSUMU MORI,^{3,4}
STEPHEN L. KINSMAN,² AND LINDA J. RICHARDS^{1,5*}

¹Department of Anatomy and Neurobiology and Program in Neuroscience,
University of Maryland School of Medicine, Baltimore, Maryland

²Department of Pediatrics, University of Maryland School of Medicine, Baltimore,
Maryland

³Department of Radiology, Division of NMR Research and Department of Biomedical
Engineering, Johns Hopkins University School of Medicine, Baltimore, Maryland

⁴F.M. Kirby Research Center for Functional Brain Imaging, Kennedy Krieger
Institute, Baltimore, Maryland

⁵University of Queensland School of Biomedical Sciences and Queensland Brain
Institute, Brisbane, Queensland, Australia

ABSTRACT

A complex set of axonal guidance mechanisms are utilized by axons to locate and innervate their targets. In the developing mouse forebrain, we previously described several midline glial populations as well as various guidance molecules that regulate the formation of the corpus callosum. Since agenesis of the corpus callosum is associated with over 50 different human congenital syndromes, we wanted to investigate whether these same mechanisms also operate during human callosal development. Here we analyze midline glial and commissural development in human fetal brains ranging from 13 to 20 weeks of gestation using both diffusion tensor magnetic resonance imaging and immunohistochemistry. Through our combined radiological and histological studies, we demonstrate the morphological development of multiple forebrain commissures/decussations, including the corpus callosum, anterior commissure, hippocampal commissure, and the optic chiasm. Histological analyses demonstrated that all the midline glial populations previously described in mouse, as well as structures analogous to the subcallosal sling and cingulate pioneering axons, that mediate callosal axon guidance in mouse, are also present during human brain development. Finally, by Northern blot analysis, we have identified that molecules involved in mouse callosal development, including *Slit*, *Robo*, *Netrin1*, *DCC*, *Nfia*, *Emx1*, and *GAP-43*, are all expressed in human fetal brain. These data suggest that similar mechanisms and molecules required for midline commissure formation operate during both mouse and human brain development. Thus, the mouse is an excellent model system for studying normal and pathological commissural formation in human brain development. © 2006 Wiley-Liss, Inc.

Key words: commissure; diffusion tensor magnetic resonance imaging; axon guidance; pioneering axons; *Npn1*; *Slit*; *Robo*

Grant sponsors: National Institutes of Health, National Institute of Neurological Disorders and Stroke; Grant numbers: R21 NS045841 (LJR); ROIAG20012 and ROIEB003543 (SM).

*Correspondence to: Linda J. Richards, University of Queensland School of Biomedical Sciences and Queensland Brain Institute, Otto Hirschfeld Building, Room 715, Brisbane, Queensland, 4072, Australia. Fax: 61-7-3365-1299. E-mail: richards@uq.edu.au

Received 16 June 2005; Accepted 7 November 2005

DOI 10.1002/ar.a.20282

Published online 13 January 2006 in Wiley InterScience (www.interscience.wiley.com).

The major forebrain commissures, which include the corpus callosum, the anterior commissure, and the hippocampal commissure, are midline axon tracts that connect the two cerebral hemispheres. Such commissural fibers must be actively guided across the midline to reach their targets in the contralateral hemisphere. When the underlying mechanisms regulating the guidance of commissural fibers fail, pathological dysgenesis of one or more commissures ensues. Agenesis of the corpus callosum (ACC) is associated with over 50 different human congenital syndromes (Jeret et al., 1987; Wisniewski and Jeret, 1991; Norman et al., 1995), resulting in a wide spectrum of anatomical, physiological, and cognitive pathologies. Furthermore, the causes of these disorders are equally varied, and to date, nearly 40 genes have been linked to callosal agenesis in humans (Richards et al., 2004b). The heterogeneous nature of these disorders suggests that a complex set of cellular and molecular mechanisms regulate commissural development. A multidisciplinary approach that provides a better understanding of how multiple forebrain commissures form will enable the development of novel therapeutic strategies to better diagnose and manage the myriad of neurological developmental disorders that manifest with commissural dysgenesis. Work in the rodent system has identified several mechanisms of axonal guidance, including the secretion of axon guidance molecules by midline glial structures (Silver et al., 1993; Shu and Richards, 2001; Shu et al., 2003a), guidance by pioneering axons from the cingulate cortex (Koester and O'Leary, 1994; Rash and Richards, 2001), as well as the expression of various regulatory genes shown to be vital for normal commissural development (reviewed in Richards et al., 2004b). However, questions remain as to whether these mouse models accurately reflect the development of commissures in humans, and the experiments in this study will seek to address this by utilizing a variety of biochemical, histological, and newly developed radiological tract tracing techniques. Here we characterize the morphological development of the commissures in the embryonic human telencephalon and determine whether the cellular structures, molecular mechanisms, and genetic systems shown to mediate callosal development in mice are also present in humans.

In both mice and humans, the development of the corpus callosum is a dynamic process that continues through gestation until well after birth. In mouse, midline fusion of the telencephalic hemispheres occurs around embryonic day 14–15 (E14–E15), and the midline zipper glia (MZG) has been proposed to mediate this process (Silver et al., 1993), which is vital for callosal formation since the fused midline serves as the substrate across which callosal fibers traverse. Following midline fusion, the corpus callosum begins to form around E15.5. Midline glial populations such as the glial wedge (GW) and the indusium griseum glia (IGG) have been shown to play critical roles in callosal development by secreting the chemorepellant molecule Slit2, which prevents callosal fibers from entering the septum, and instead guides them across the midline and into the contralateral hemisphere (Shu and Richards, 2001; Shu et al., 2003a). The existence of these glial structures in the human embryonic brain has recently been demonstrated by Lent et al. (2005). The subcallosal sling, first identified by Silver et al. in 1982, is situated at the corticoseptal border and has also been shown to play a role in callosal formation (Silver and Ogawa, 1983). Mid-

line glial cells also mediate the guidance of other forebrain commissures such as the optic chiasm and the anterior commissure (Marcus et al., 1995; Wang et al., 1995; Cummings et al., 1997). In mouse, the first callosal axons, known as pioneering axons, project homotopically from the cingulate cortex (Koester and O'Leary, 1994; Rash and Richards, 2001) and form the dorsal portion of the developing corpus callosum (Ozaki and Wahlsten, 1992). Semaphorins and their receptors the neuropilins have been shown to guide cortical axons as they first leave the cortical plate (Bagnard et al., 1998; Polleux et al., 1998). We have recently found that neuropilin 1 (Npn1) labels the callosal pioneering axons in mouse (Plachez et al., 2004) and here we examine the protein expression of Npn1 in developing human brains.

We hypothesize that the complex mechanisms regulating callosal formation in mouse have been evolutionarily conserved, and that similar cellular structures and molecular regulatory processes operate to guide commissural development in the human fetal brain. To test this hypothesis, we have analyzed 14 human fetal brains ranging from 13 to 19 weeks of gestation. We utilized both conventional histological methods, as well as the newly developed diffusion tensor magnetic resonance imaging (DTMRI) method to characterize the morphology of major axonal tracts during fetal development (Table 1). In addition, we have analyzed the formation of multiple midline glial populations, the subcallosal sling, and pioneering axons in the human embryonic brain, and the expression of developmentally important genes by both Northern blot and immunohistochemical analysis. The data from these experiments will demonstrate whether mouse models of normal and pathological commissural development are applicable to the human system.

MATERIALS AND METHODS

Human fetal tissue was obtained from the National Institute of Child Health and Human Development (NICHD) Brain and Tissue Bank for Developmental Disorders, at the University of Maryland, Baltimore School of Medicine, under contract N01-HD-4-3368. Whole embryonic brains from a wide developmental period were used (see Table 1 for summary). Brains used for immunohistochemical analyses were immersion-fixed in 4% paraformaldehyde (PFA) for 4 weeks, with fresh 4% PFA changed every week prior to sectioning and analysis. One unfixed brain was kept frozen in dry ice and utilized for RNA extraction in order to conduct the Northern blot analysis shown in Figure 6. Postfixation, brains were scanned by DTMRI at Johns Hopkins University School of Medicine. Following scanning, fixed brains were immersed in 10–30% sucrose in 4% PFA for 2–3 days until they sank in the solution, then frozen in liquid 2-methylbutane at -20°C . Frozen brains were serially sectioned at 80 μm coronally on a freezing microtome. Sections were stored in a cryoprotectant solution (Watson et al., 1986) and were then transferred into a $1\times$ phosphate-buffered saline (PBS; pH 7.4) just prior to immunohistochemistry.

DTMRI

Diffusion tensor magnetic resonance imaging is capable of visualizing all major axon tracts in the brain and has the added benefit of color-coding these fiber tracts by direction (i.e., commissural fibers, all of which run medio-

TABLE 1. Summary of fetal human brains analyzed

Age	Case #	GFAP	NcuN	Nfia	CR	NF	GAP43	Npn1
13	4501*	x	x			x	x	
14	1921*	x	x			x	x	
15	1885*	x	x	x	x		x	
	1887	x	x	x	x	x		
16	1775				x			
	1886*	x	x	x	x			
	1531	x		x	x			
17	1532*	x	x					
	1777		x		x	x	x	
	1770	x		x				x
	1854	x	x			x		
	1755 [§]							
18	4567*							
19	4503*	x	x	x	x	x		
	1853	x	x			x		

Age is measured in gestational weeks.

GFAP, Glial Fibrillary Acid Protein; CR, Calretinin; NF, Neurofilament; Npn1, Neuropilin1.

*, brains analyzed by DTMRI. 1755[§], this brain was frozen fresh and its tissue was utilized for Northern blot analysis (Fig. 6).

laterally, will be of the same color, red in the case of our images). The MRI data are processed and transformed into a three-dimensional representation of the scanned brain, and through the use of DTIStudio software, any section of the brain can be analyzed through three brain axes: coronal, sagittal, or horizontal. Three-dimensional multiple echo diffusion tensor imaging (DTI) was performed in both 11.7 and 4.7 Tesla (T) Bruker magnetic resonance scanners to acquire high resolution and high signal-to-noise ratio (SNR) images. Fetal brains between 14 and 16 weeks of gestation were scanned in an 11.7 T Bruker scanner with a Bruker micro 2.5 volume coil. Brains 17 weeks and older were scanned in a 4.7 T Bruker scanner with an 80 mm diameter Bruker birdcage volume coil. Fetal brains were immersed in PBS and placed in custom-made chambers during the scan.

For diffusion tensor imaging, a set of diffusion-weighted images were acquired in six linearly independent directions. The imaging sequence has been previously described by Mori and van Zijl (1998). The diffusion of water molecules in biological tissues can be approximately characterized by a three-by-three symmetric matrix, the so-called diffusion tensor, and can be visualized as an ellipsoid that represents the properties of water molecule diffusion in each voxel. For isotropic diffusion (e.g., free diffusion), the shape of the ellipsoid becomes a sphere, and for anisotropic diffusion (e.g., restricted diffusion in the white matter), the shape becomes highly elongated, with the longest axis aligned to the orientation of axonal fibers. The elements within a tensor are water diffusion constants along the x, y, z, xy, xz, and yz directions. The diffusion tensor can be diagonalized to generate three pairs of eigenvector and eigenvalue, which correspond to the three axis of the ellipsoid and their lengths. To estimate diffusion tensor, a set of diffusion-weighted images were acquired in seven linearly independent directions (Basser et. al., 1994). The diffusion tensor was calculated using a log-linear fitting method from these seven images, and three pairs of eigenvalues and eigenvectors were calculated for each voxel. The eigenvector associated with the largest eigenvalue was referred to as the primary eigenvector and represents the orientation of axonal fibers. For

the quantification of anisotropy, fractional anisotropy (FA) was used (Pierpaoli and Basser, 1996). Using primary eigenvector and FA, color maps were calculated. In the color map images, the red, green, and blue value of each pixel was defined by the orientation of its primary eigenvector, and the intensity was proportional to the FA so that white matter regions were brighter. Red was assigned to the fiber orientation along the medio-lateral axis, green to the rostral-caudal axis, and blue to the dorsal-ventral axis.

Immunohistochemistry

All immunohistochemistry was performed on floating sections. Fetal brain sections were rinsed three times, 10 min each time, in PBS and were then blocked in 2% normal goat serum [used for rabbit antigial fibrillary acidic protein (GFAP; Dako), neuropilin1 (Npn1; a gift from Dr. D. Ginty, Johns Hopkins University), Nfia (Geneka), and calretinin (CR; Swant) antibodies] or donkey serum [used for mouse anti-NeuN (Chemicon) and growth cone-associated protein 43 (GAP43; Chemicon) antibodies] and 0.2% Triton-X in PBS for a period of 2 hr. This was followed by overnight incubation with primary antibody diluted in the blocking solution at varying concentrations: GFAP at 1:30,000, Npn1 at 1:50,000, Nfia at 1:20,000, CR at 1:5,000, GAP43 at 1:100,000, and NeuN at 1:3,000. On the following day, the sections were washed with PBS three times, 20 min each time, then incubated with biotinylated goat antirabbit (for GFAP, Npn1, Nfia, and CR) or donkey antimouse (for GAP43 and NeuN) secondary antibodies (Jackson ImmunoResearch) diluted at 1:600 in PBS with 0.2% Triton-X100 for 1 hr. After another three washes in PBS, the sections were incubated in an avidin/biotin solution (ABC kit; Vector) at 1:500 in PBS with 0.2% Triton-X100 for 1 hr. Following three washes in PBS, the sections were immersed in a nickel-DAB solution (0.02% DAB and 2.5% nickel sulfate in 0.175 M sodium acetate) activated with 0.01% H₂O₂ until a dark-purple precipitation formed. Finally, sections were mounted onto gelatinized glass slides, dehydrated through increasing concentrations of ethanol, immersed

in two changes of HistoClear solution, and coverslipped with DPX mounting medium.

Northern Blot Analysis

RNA was extracted from the cortex and the ventral forebrain (including the hippocampus and the diencephalon) of one fetal brain aged 17 gestational weeks (case 1755). From this tissue, total RNA was extracted using TRIzol (Gibco), followed by mRNA extraction using the GenElute mRNA miniprep kit (Sigma). Both total RNA and mRNA were used in the Northern blot analysis. The probes used for this analysis were generated by RT-PCR, starting with the reverse transcription of the RNA using random primers. This was followed by PCR reaction using specific primers for the genes of interest. The accession numbers (AN) and forward primer (FP) and reverse primer (RP) sequences for each gene are as follows: for *hSlit1* (AN AB017167), FP of 5'-GTACTTCATTCAGGCACG-3' and RP of 5'-GGGAATCTGCCGCAAAAAG-3'; for *hSlit2* (AN AF133270), FP of 5'-GCTCAACAAAATCCCGGAG-3' and RP of 5'-CTTGTTGCTACATCGGACG-3'; for *hSlit3* (AN AB017169), FP of 5'-CATCTGCAATGCCAACTC-3' and RP of 5'-GCGGAACCTTCTTGCTCTTG-3'; for *hRobo1* (AN NM_002941), FP of 5'-GGTACACCTGCATTGCATC-3' and RP of 5'-CCACACTGTTTTGGCTGG-3'; for *hRobo2* (AN XM_031246), FP of 5'-CAGGCAAGTGCAGAAAGAG-3' and RP of 5'-GGCTGCATCCACAGTTTTG-3'; for *hRobo3* (AN AY509035), FP of 5'-GTACATGCCAATGTGCAG-3' and RP of 5'-CCAACATTGTCCAGCTTCC-3'; for *hNetrin1* (AN HSU75586), FP of 5'-GGCAAACCTGCAACCAAAC-3' and RP of 5'-GCTTTTATCGGCCACGATGC-3'; for *hDCC* (AN HOMO HSDCCG), FP of 5'-CCTCCACCAAGTTTTACCTG-3' and RP of 5'-GTAAGCCACAACCTCGAAAG-3'; for *hEMX1* (AN HOMO HSEM1), FP of 5'-ACCGGGACCCTCTCCATTTC-3' and RP of 5'-TCGATGTCCTCCCATTGGC-3'; for *hNfia* (AN XM_046827), FP of 5'-GTGTCACAGACACCAATAGC-3' and RP of 5'-CCCATTGGGATTGAGGAACC-3'; and for *hGAP43* (AN NM_002045), FP of 5'-GCCTAAACAAGCCGATGTG-3' and RP of 5'-GAGAGAGGAAAGTGGACTCC-3'. cDNA fragments of between 400 and 700 bp were generated and radiolabeled with ³²P; 20 μg of total RNA or 0.5 μg of mRNA per well was loaded onto a 1.2% agarose gel containing 2.2 M formaldehyde, separated by electrophoresis, and transferred to a nylon membrane using a standard protocol. The membrane was then incubated in a prehybridization solution for 2 hr, when the ³²P-labeled probe was added, and incubation was continued for 12–16 hr. Following incubation, the membrane was washed in a series of sodium citrate buffer (SSC) solutions containing 0.1% SDS at 68°C before being dried and exposed to X-ray film at -70°C for 24 hr.

Preparation of Figures

Data from DTMRI were visualized using DTI-Studio software (version 1.03), from which desired brain slice images were exported. Low-power photographs of immunostained brain sections were taken on a Nikon SMZ 1500 digital camera connected to a Nikon dissecting microscope, while high-power photographs of the same sections were taken using a PhaseOne digital camera connected to a Leica light microscope.

RESULTS

Morphological Development of Axonal Tracts

Figures 1 and 2 demonstrate the general morphology of major axon tracts in the human embryonic brain utilizing different imaging modalities. Figure 1 displays the distribution of the major forebrain commissures in human fetal brains at three different developmental stages by DTMRI analysis, which allows for tract tracing on a global scale. The axon bundles traced by DTMRI are color-coded with different colors denoting the direction of the axon tracts. The colors are arbitrarily assigned and in our analysis are as follows: red denoting fibers running medio-laterally, green denoting fibers running rostro-caudally, and blue denoting fibers running dorso-ventrally. Analysis of the DTMRI scans demonstrates that major forebrain commissures (color-coded red), as well as other major axon tracts, can be clearly demarcated in the developing human brain. At 13 gestational weeks (Fig. 1A–D), both the anterior commissure and optic chiasm are well developed (Fig. 1A), while the corpus callosum has yet to form (arrow in Fig. 1A–C), and in fact midline fusion of the cerebral hemispheres has yet to occur (Fig. 3A). The corpus callosum does form at 14 gestational weeks (data not shown), and by 15 gestational weeks (Fig. 1E–H), the corpus callosum can be easily identified in both coronal (Fig. 1E) and horizontal (Fig. 1G) sections. Furthermore, the major forebrain commissures (in order from dorsal to ventral: corpus callosum, hippocampal commissure, and the anterior commissure), as well as the optic chiasm, and the pontine decussation (pseudocolored red) and the pyramidal tract (pseudocolored blue) can be observed simultaneously in a mid-sagittal section (Fig. 1F). While the same structures are also present at 18 and 19 gestational weeks (Fig. 1I–O), several developmental changes become apparent. Beyond a simple size difference, analysis of sagittal images (Fig. 1J and M) reveals that the corpus callosum extends far more caudally at 18 and 19 weeks compared to 15 weeks of gestation, with the development of the splenium beginning at 18 weeks. Furthermore, the hippocampal commissure, located just ventral to the corpus callosum, also appears to undergo significant development during this period. At 15 gestational weeks, the cross-sectional area of the hippocampal commissure is similar to that of the anterior commissure and the optic chiasm (Fig. 1F). However, by 18 gestational weeks, it has markedly increased in size and is especially prominent in horizontal view (Fig. 1K).

In addition to DTI, conventional histological analyses were performed to examine axonal structures in the fetal brain, utilizing immunohistochemistry with a nickel-DAB chromagen. Figure 2 shows coronal sections from a human embryonic brain, aged 17 gestational weeks, immunostained with growth cone-associated protein 43 (GAP43), an axon-specific marker. Notably, the corpus callosum, hippocampal commissure, and anterior commissure, as well as the internal capsule, can all be delineated in Figure 2C. The data verify the anatomical location and size of these tracts depicted in Figure 1 by DTMRI analysis.

Key Midline Structures Are Present in Developing Human Brain

In order to determine whether important midline structures shown to play key roles in regulating commissural development in mouse are also present in the developing

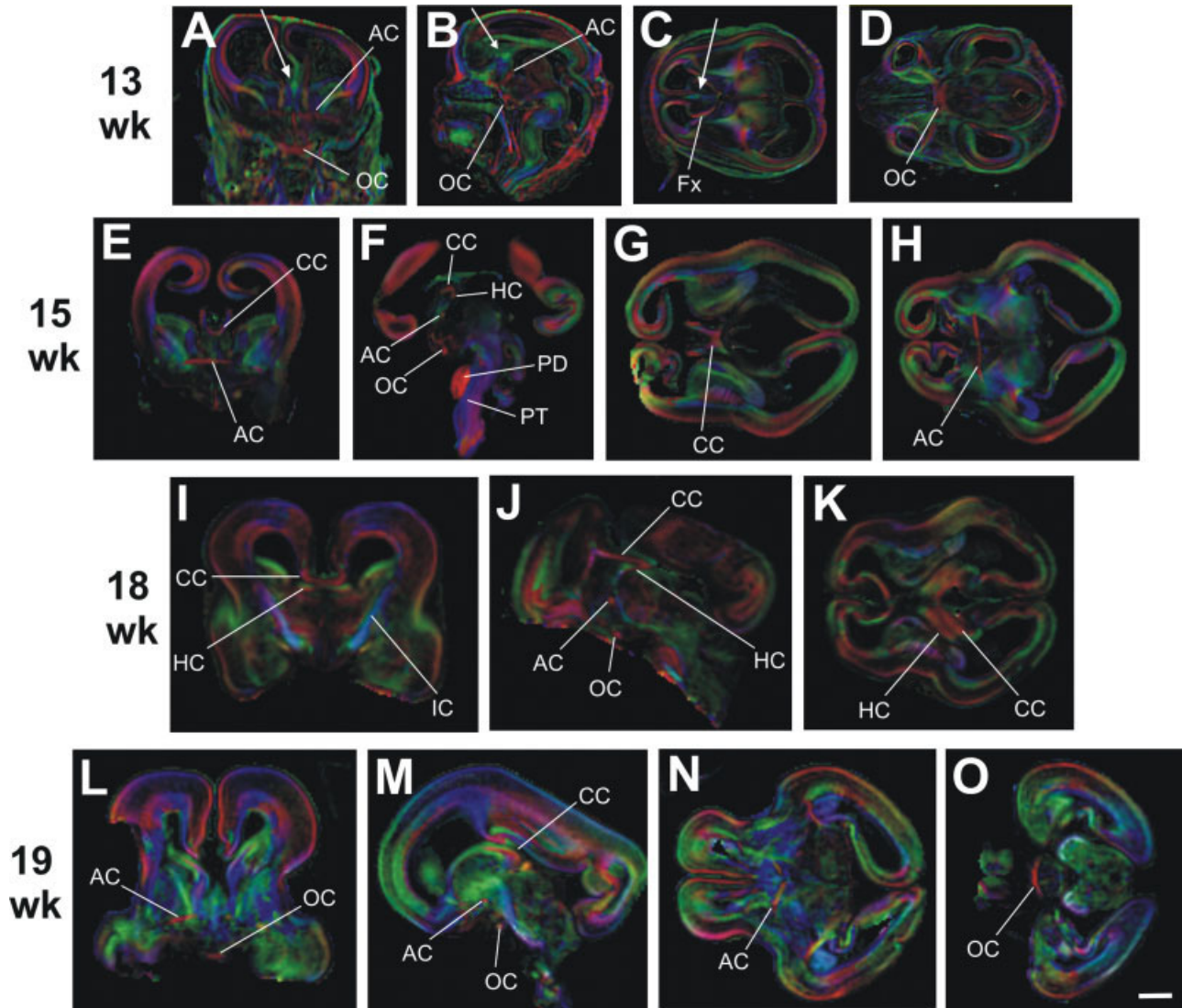


Fig. 1. DTMRI analysis of human fetal brain. DTMRI sections of human fetal brains at 13 (A–D), 15 (E–H), 18 (I–K), and 19 (L–O) weeks of gestation, taken in coronal (A, E, I, L), sagittal (B, F, J, M), and horizontal (C, D, G, H, K, N, O) orientations. The fiber tracts visualized by DTMRI are pseudocolored according to their orientation, with fibers running medio-laterally colored red, fibers running rostrocaudally colored green, and fibers running dorsoventrally colored blue. For sagittal and horizontal

sections, rostral is to the left. DTMRI successfully visualized all major forebrain commissures, as well as other major axonal structures in the brain at 15, 18, and 19 gestational weeks and also demonstrate that the corpus callosum has yet to form at 13 gestational weeks (arrow in A–C). CC, corpus callosum; AC, anterior commissure; HC, hippocampal commissure; OC, optic chiasm; PD, pontine decussation; PT, pyramidal tract; IC, internal capsule; Fx, fornix. Scale bar = 3 mm.

human brain, a series of immunohistochemical assays were performed on coronal sections from human embryonic brains ranging from 13 to 19 weeks of gestation [a previous complimentary study utilized brains from 19–23 weeks (Rezaie et al., 2003)]. Specific antibodies against the midline glial populations (the GW and IGG), the subcallosal sling, and the pioneering axons of the corpus callosum were utilized to determine whether these structures are present during human development.

In Figure 3, fetal brains ranging from 13 to 19 weeks of gestation were analyzed by GFAP immunohistochemistry for the presence of the GW and IGG. These experiments demonstrate that by week 14 of gestation, both the GW and the IGG are present (Fig. 3F), flanking either side of

the developing corpus callosum. Between 13 and 19 weeks of gestation, the development of these midline glial populations occurs both at a gross structural level and at a cellular level. Grossly, glial cells densely populate the ventricular zone of the midline at 14 gestational weeks, spreading along the midline as well as in the septum and the developing neocortex. Over the next few weeks, glial cells coalesce at the corticoseptal boundary into the glial wedge, IGG, and midline zipper glia (Figs. 3H, K, and N). At a cellular level, radial glial cells (Fig. 3I) of the glial wedge begin to differentiate into astrocytes (Fig. 3L) beginning at 14 gestational weeks and continuing until at least 19 gestational weeks in our study and up to 23 weeks as previously reported (Rezaie et al., 2003).

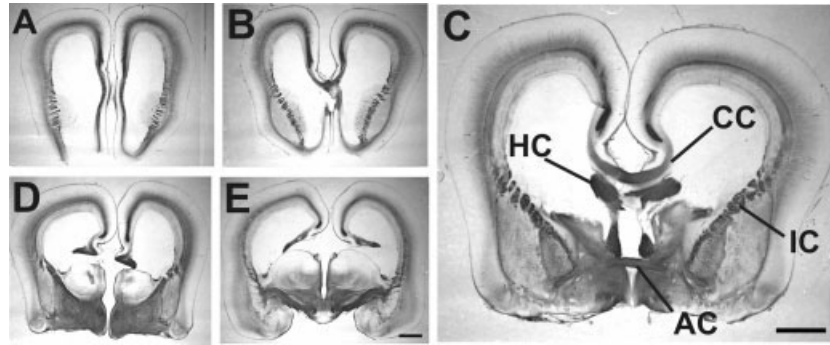


Fig. 2. Axonal tract morphology at 17 gestational weeks. Immunostaining of coronal sections from human fetal brain aged 17 gestational weeks with GAP43 antibody, a marker of axon tracts, and visualized by a nickel-DAB chromagen. The sections progress from rostral to caudal (A–E), and three major forebrain commissures, as well as the internal

capsule, can all be delineated in C, which is enlarged compared to the other sections. AC, anterior commissure; CC, corpus callosum; HC, hippocampal commissure; IC, internal capsule. Scale bars in E = 3 mm in A, B, D, and E; in C = 3 mm.

Several markers are known to be specific for the subcallosal sling in mouse, including NeuN, Nfia, and calretinin (CR) (Shu et al., 2003c), and all three were used to examine the presence of the subcallosal sling in coronal sections of human fetal brains aged 13, 15, and 17 weeks of gestation (Fig. 4). NeuN-positive cells were observed near the midline at 13 weeks of gestation (Fig. 4A–C; arrow in C). Two populations of cells began to form at the midline by 15 weeks of gestation: one above the corpus callosum (Fig. 4I) and one below (Fig. 4F). The first cluster of cells, densely stained with NeuN, formed bilaterally at the corticoseptal boundary (Fig. 4F), and over time more cells within this population were observed closer to the midline (Fig. 4L; labeled with calretinin), suggesting that the population of cells may be migrating toward the midline as they do in mouse (Shu et al., 2003c). At the same developmental stage, a second Nfia-positive population was evident more dorsally in the region of the indusium griseum (Fig. 4H, arrow in 4I). GFAP-positive cells were also observed within the subcallosal sling region (arrows in Fig. 3N and O). These data provide evidence that the subcallosal sling is present in humans and contains both neurons and mature glial cells.

Pioneering axons from the cingulate cortex are the first axons to cross the midline as part of the corpus callosum in mice (Koester and O'Leary, 1994; Rash and Richards, 2001). To investigate the presence of pioneering axons in the human fetal brain, we used a marker called neuropilin 1 (Npn1), which labels the pioneering axon population in mouse (Plachez et al., 2004). Furthermore, within the developing corpus callosum, there is a loose topography with respect to the origin of the fibers in the corpus callosum; more medially located neurons project in the dorsal region and more laterally located neurons project in the ventral region (Ozaki and Wahlsten, 1992). In coronal sections of human fetal brain at 17 weeks of gestation, axon fibers within corpus callosum are labeled with Npn1 (Fig. 5A), and higher-powered views of these axons reveal that they originate from the cingulate cortex of one hemisphere and project homotopically to the contralateral cingulate cortex as they do in mice (arrows in Fig. 5C) (Plachez et al., 2004). These data indicate that the developing human corpus callosum contains Npn1-positive axons analogous to the pioneering axons found in mice (Plachez et al., 2004).

Expression of Commissural Regulatory Genes in Developing Human Brain

The actions of secreted guidance molecules (such as Slit2) and their receptors (such as Robo1 and Robo2) play key roles in the guidance of commissural axons. Knockout studies in mice have demonstrated the involvement of a number of different genes in callosal development (reviewed in Richards, 2002; Richards et al., 2004b). These genes include guidance factors such as Slit2 (Bagri et al., 2002) and Netrin1 (Serafini et al., 1996), receptor molecules such as Robo (Richards et al., 2004a), DCC (Fazeli et al., 1997), and Npn1 (Gu et al., 2003), transcription factors such as Nfia (Shu et al., 2003b), Emx1 (Qiu et al., 1996; Yoshida et al., 1997), and Emx-2 (Pellegrini et al., 1996; Yoshida et al., 1997; Martins et al., 2004), as well as GAP43 (Shen et al., 2002). Knockouts in any of these genes results in either complete absence or severe dysgenesis of the corpus callosum. To determine whether these genes shown to play key regulatory roles in commissural development in the rodent are also expressed in the developing human brain, we utilized RT-PCR to generate cDNA probes specific to the human homologs of these genes and used them in a Northern blot analysis with tissue derived from a 17-gestational-week brain (Fig. 6). The genes for which we generated cDNA probes include the guidance molecule *Netrin1*, its receptor *deleted in colon cancer (DCC)*, the guidance molecules *Slit1*, *Slit2*, and *Slit3*, and their receptors *Robo1* and *Robo2*, the transcription factors *Nfia* and *Emx1*, and the axon growth and guidance molecule *GAP43*.

Cortical expression was analyzed for each gene, and the cDNA probes were applied against both total RNA (lane 1) and mRNA (lane 2), except for *Slit3*, for which only total RNA was analyzed. Expression was analyzed separately in tissue from the dorsal neocortex and tissue from the ventral and caudal forebrain, which included the ganglionic eminences, the hippocampus, and the diencephalon. The ventral/caudal tissue was analyzed for the expression of the secreted guidance molecules *Netrin1*, *Slit1*, *Slit2*, and *Slit3*, since all of these genes are known to be more highly expressed in the ventral forebrain; again, both total RNA (lane 3) and mRNA (lane 4) were used. The results from the Northern blot analyses suggest that the 10 genes analyzed are all expressed at this stage of fetal brain

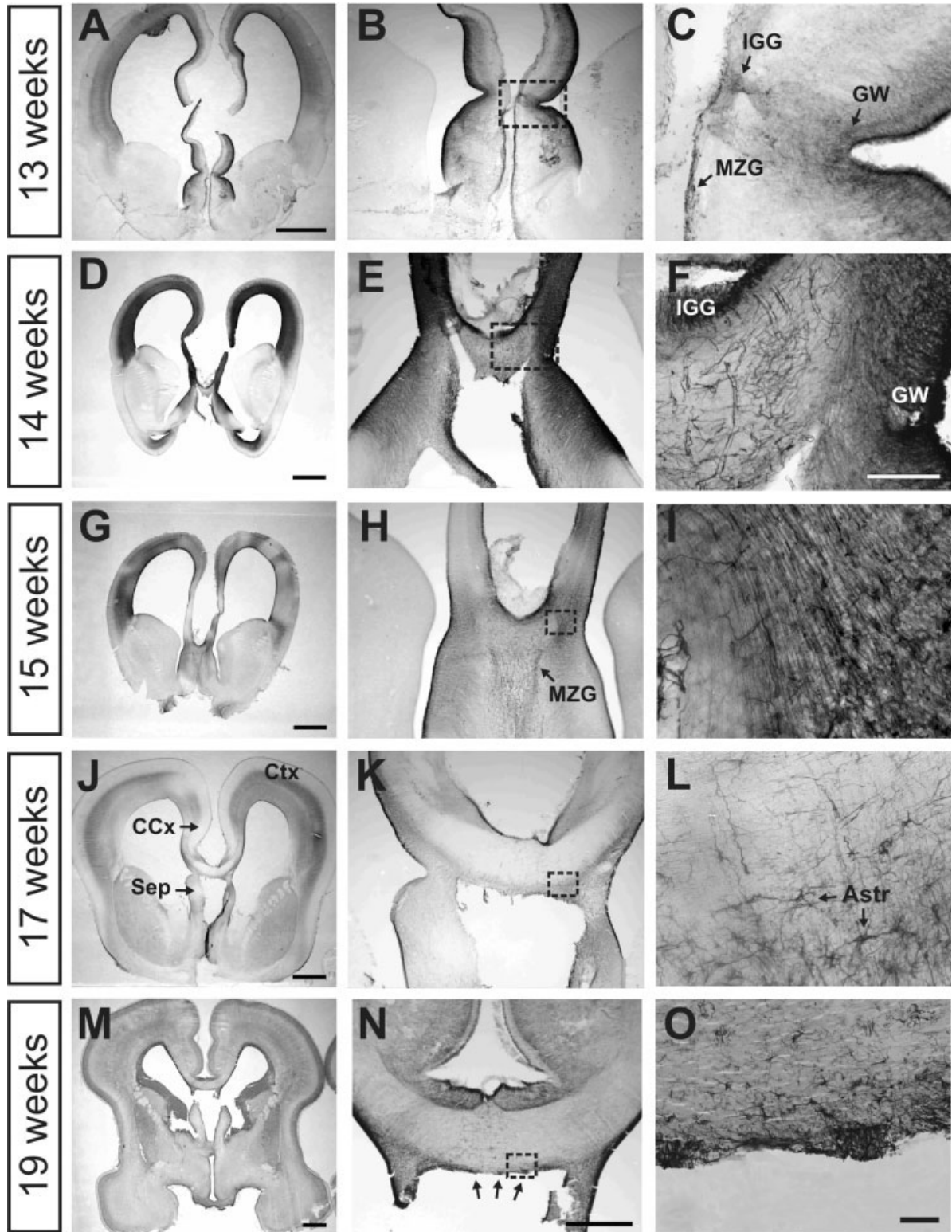


Fig. 3. Development of midline glial structures in human fetal brain. Immunostaining of coronal sections from five separate human fetal brains aged 13 (A–C), 14 (D–F), 15 (G–I), 17 (J–L), and 19 (M–O) gestational weeks with GFAP antibody, and visualized by a nickel-DAB chromagen at low (left), intermediate (middle), and high (right) levels of magnification. GFAP-positive glial wedge and IG cells are present and persists until at least 19 gestational weeks. Glial wedge cells form a

radial glial scaffold initially (I) and later develop into astrocytes (L and O). Boxes in B, E, H, K, and N denote areas of magnification in C, F, I, L, and O, respectively. GW, glial wedge; IG, indusium griseum glia; MZG, midline zipper glia; Ctx, cortex; CgC, cingulate cortex; Sep, septum; Astr, astrocytes. Scale bars in A, D, G, J, and M = 3 mm; in N = 1 mm in B, E, H, K, and N; in F = 300 μ m in C and F; in O = 50 μ m in I, L, and O.

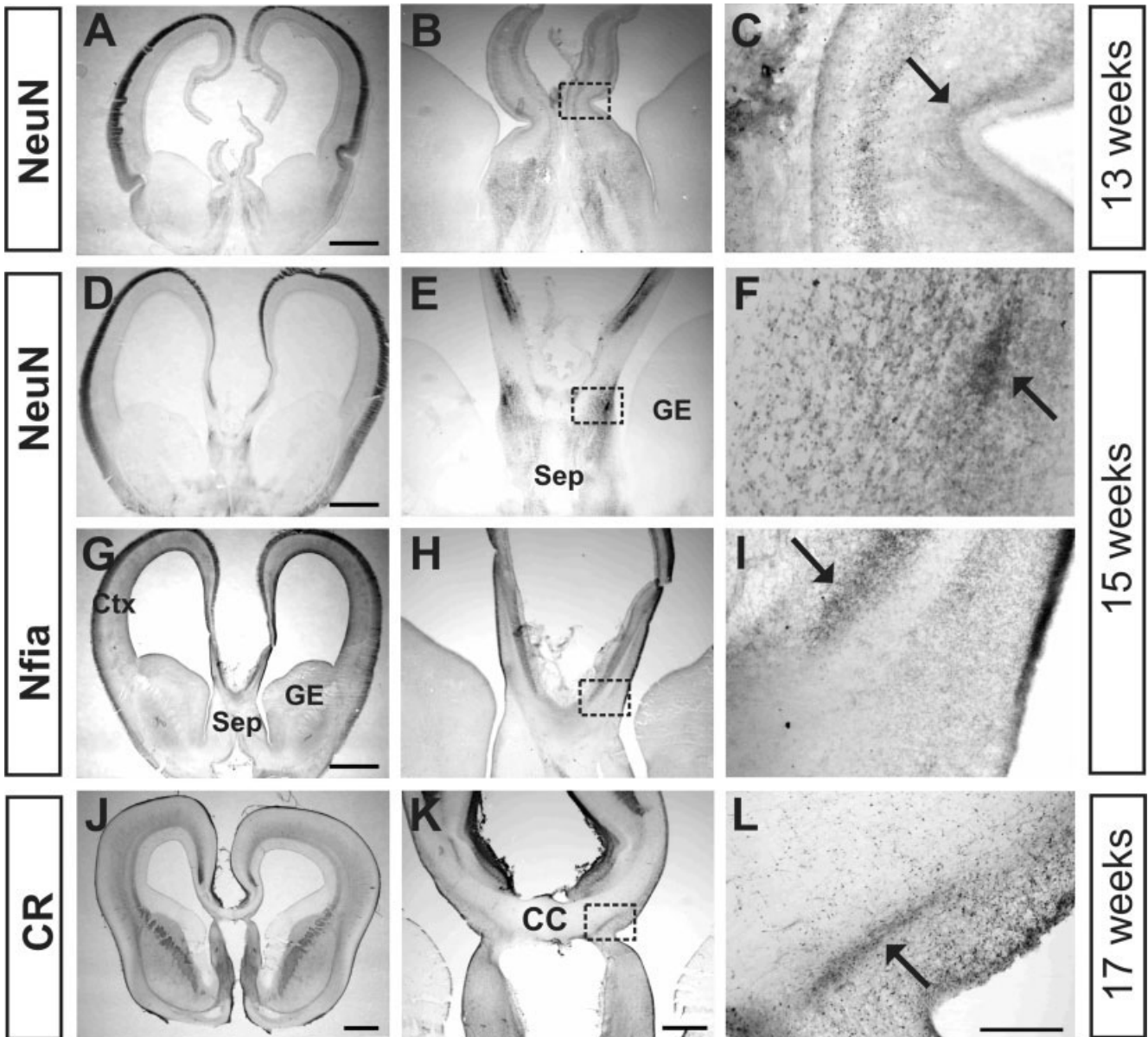


Fig. 4. Subcallosal sling development in human fetal brain. Immunostaining of coronal sections from four separate human fetal brains aged 13 (A–C), 15 (D–F), and 17 (J–L) gestational weeks with NeuN (A–F), *Nfia* (G–I), or calretinin (CR; J–L) antibodies, and visualized by a nickel-DAB chromagen at low (left), intermediate (middle), and high (right) levels of magnification. Sling cells originate from bilateral cell clusters (arrow in F) at 15 weeks of gestation and migrate toward the midline, forming a sling

by 17 gestational weeks (arrow in L), while a dorsal population of *Nfia*-positive cells is also apparent at 15 gestational weeks (arrow in I). CC, corpus callosum; GE, ganglionic eminence; Ctx, cortex; Sep, septum. Boxes in B, E, H, and K denote areas of magnification in C, F, I, and L, respectively. Scale bars in A, D, G, J = 3 mm; in K = 1 mm in B, E, H, and K; in L = 300 μ m in C, F, I, and L.

development. For the Slit receptors *Robo1* and *Robo2*, paired bands measuring 6 and 8 kb, and 7 and 9.5 kb, respectively, are observed in cortex, compared to the reported sizes of 8 kb for murine *Robo1*, and 7 and 9.8 kb for murine *Robo2* (Sundaresan et al., 2004). For the Netrin1 receptor *DCC*, a single band at 10 kb is observed in cortex, while the reported sizes of *hDCC* are 7.5 and 10 kb (Meyerhardt et al., 1997). For the transcription factor *Emx1*, a pair of bands was observed in cortex, measuring 1.8 and 4 kb. The sizes of these transcripts have been reported as

3.3 and 5.8 kb in zebrafish (Morita et al., 1995), indicating an evolutionary difference in transcript size between fish and humans. The other transcription factor analyzed, *Nfia*, exhibited three bands on Northern blot analysis using extracted cortical mRNA (lane 2), measuring at 1.8, 5.4, and 9.8 kb, compared to its reported sizes of 5 and 10 kb (Misawa and Yamaguchi, 2002). Finally, the Northern blot for *GAP43* demonstrated a strong band at 1.8 kb, similar to its reported size of 1.4 kb in the human (Edsjo et al., 2004).

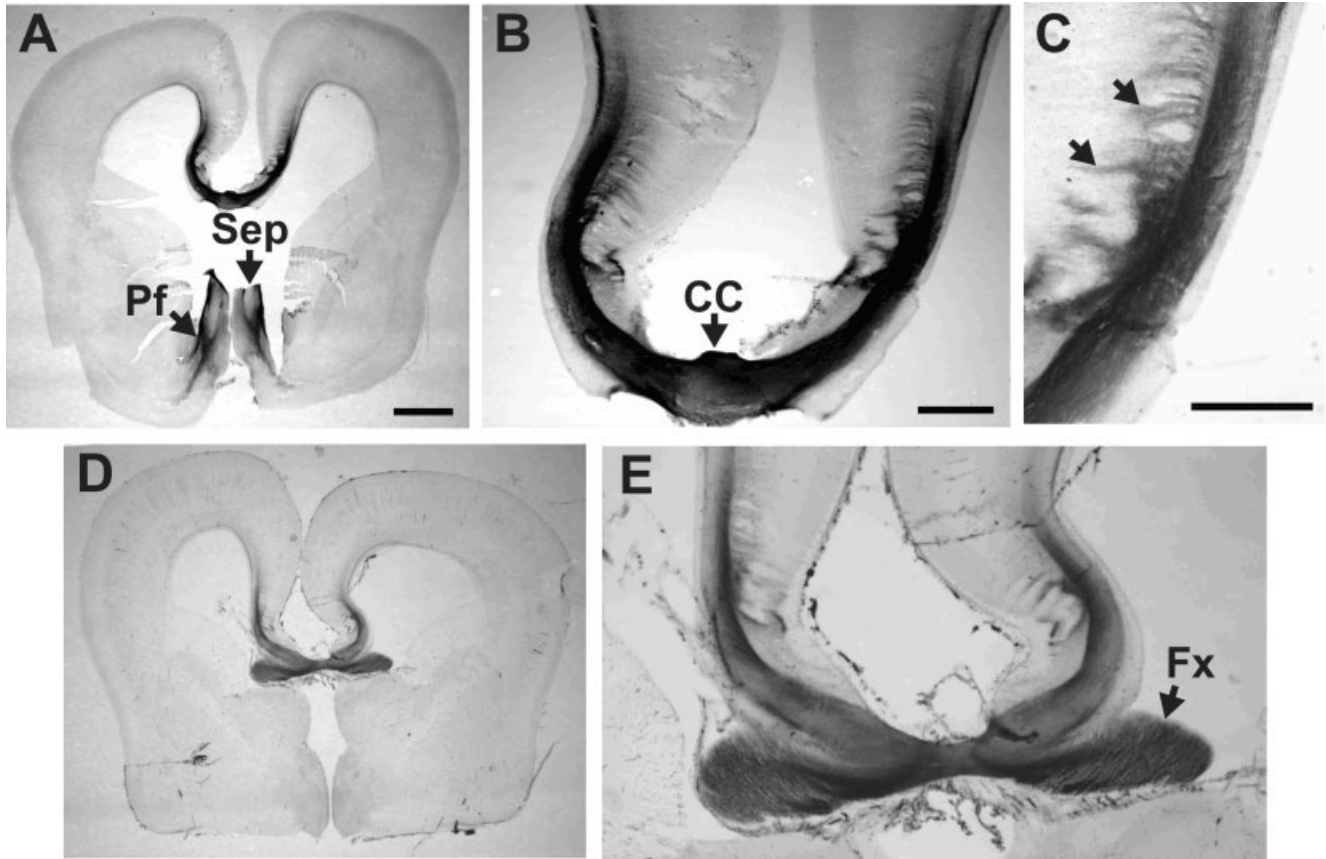


Fig. 5. Human pioneering axons at 17 gestational weeks. Immunostaining of coronal sections from a human fetal brain aged 17 weeks of gestation with neuropilin 1 (Npn1) antibody, and visualized by a nickel-DAB chromagen. Npn1 specifically labels axon projections derived from neurons of the cingulate cortex (A–C; arrows in C; B and C are higher power views of A), which then form homotopic projections to the con-

tralateral cingulate cortex. Npn1-positive cingulate axons also project between the septum and cingulate cortex via the perforating pathway (arrow in A labeled Pf), and to the hippocampus via the fornix (arrow in E). CC, corpus callosum; Sep, septum; Pf, perforating pathway; Fx, fornix. Scale bars in A = 3 mm in A and D; in B = 1 mm in B and E; in C = 1 mm.

The guidance molecule genes have a different general expression pattern. *Netrin1*, the ligand for DCC, is more highly expressed in total RNA extracted from ventral/caudal forebrain (lane 3) than total RNA from cortex (lane 1). Its band is measured at 6 kb, which is equal to the size of the rat *Netrin1* gene (Ellezam et al., 2001). In contrast, *Slit1* is expressed in both the dorsal neocortex and the ventral/caudal forebrain, exhibiting bands of 5.5 and 8.5 kb. *Slit2* and *Slit3*, however, are also more highly expressed in ventral/caudal forebrain (lane 3) compared to cortex (lane 1) and exhibit bands at 4 and 8 kb for *Slit2* and 9.5 kb for *Slit3*. Itoh et al. (1998) have reported the sizes of human *Slit1*, *Slit2*, and *Slit3* to be 5.9 and 8.4, 8, and 5.5 and 9.5 kb, respectively.

DISCUSSION

At present, the large number of human developmental disorders that exhibit ACC, as well as other midline commissural defects, represent a black box where the crucial mechanisms leading to these final pathological phenotypes remain unknown. The experiments in this report have utilized molecular, histological, and imaging techniques to investigate the morphological, cellular, and mo-

lecular characteristics of human callosal development, and our results indicate that the same guidance mechanisms and molecules known to be required for mouse commissural formation are also present in the human fetal brain. As a first step, these results may lead to a greater understanding of human commissure formation and how pathological malformations of the corpus callosum arise in humans.

Development of Axonal Tracts in Human Fetal Brain

In humans, callosal fibers have been reported to cross the midline at approximately 13 gestational weeks (Hewitt, 1962; Rakic and Yakovlev, 1968). However, our data suggest that axons do not cross a fused midline until 14 gestational weeks (Fig. 3D), and no discernable corpus callosum, or even midline fusion, was observed at 13 gestational weeks (Figs. 1A and 3A). There may be several explanations for this minor discrepancy. None of the prevailing methods for the dating of a human fetus, which include dating by date of the last menstrual period, the use of ultrasound to perform measurements in utero, and measurement of crown-rump length of postmortem tissue,

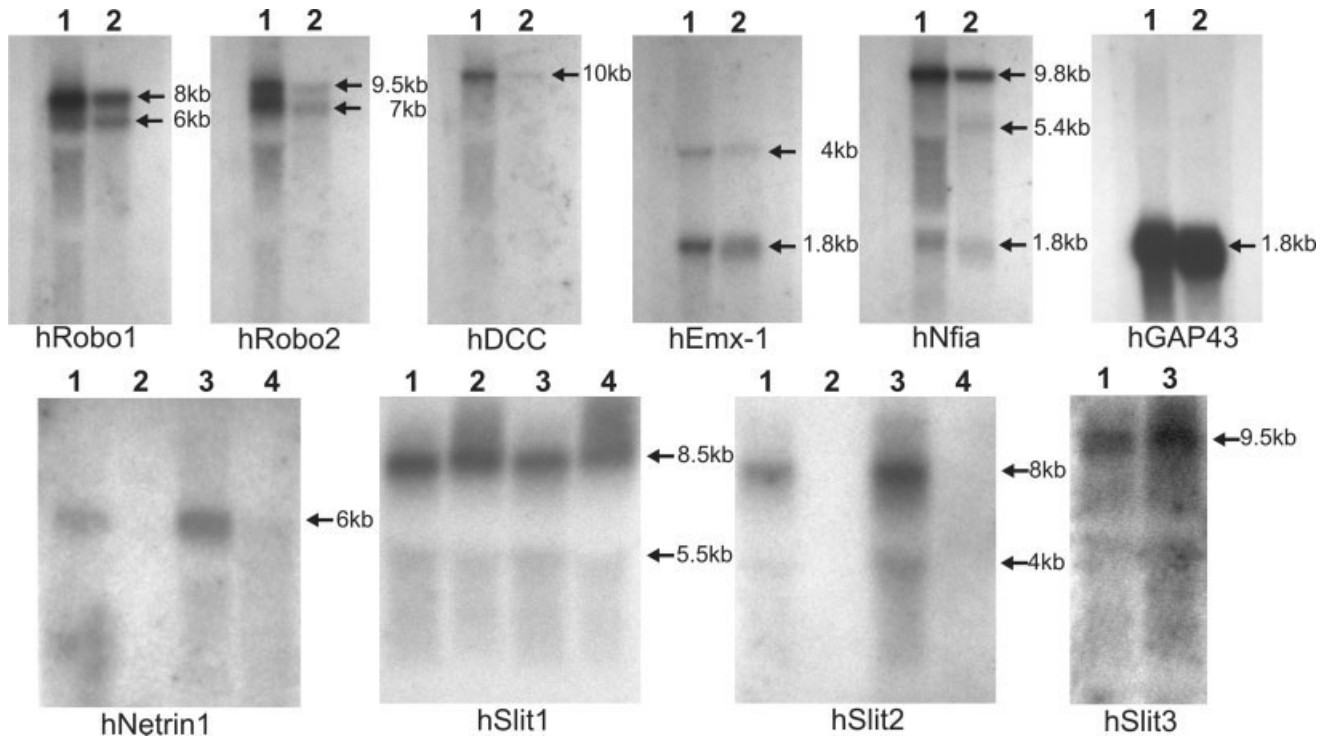


Fig. 6. Northern blot analysis of key axonal guidance genes. Northern blot analysis of the expression of various transcripts of guidance molecules (*DCC*, *Netrin1*, *Robo1*, *Robo2*, *Slit1*, *Slit2*, and *Slit3*), regulatory genes (*Nfia* and *Emx1*), and *GAP43* in human fetal brain aged 17 gestational weeks. Lane 1, total RNA from cortex; lane 2, mRNA from cortex; lane 3, total

RNA from ventral forebrain; lane 4, mRNA from ventral forebrain. Note the increased expression of guidance molecules *Netrin1*, *Slit2*, and *Slit3* in ventral/caudal forebrain compared to dorsal neocortex (compare lanes 3 and 1).

are considered to be extremely accurate. The early studies by Hewitt (1962) and Rakic and Yakovlev (1968) utilized embryonic crown-rump length to estimate gestational age. In contrast, the NICHD Brain and Tissue Bank for Developmental Disorders, which provided and dated the human tissue analyzed in this report, utilizes maternal ultrasound and foot-length measurements to determine embryonic age, which may account for the discrepancy. Another possible explanation would be an inherent variability of human brain development between individual fetuses. Furthermore, access to well-preserved human brain tissue is highly limited: only one 13- and one 14-week-old brain have thus far been analyzed in our cohort. Hence the examination of multiple specimens at 13 weeks of gestation and younger is required to date the crossing of the first callosal fibers in humans definitively.

We utilized two different methods to examine the morphology of major fiber tracts in the brain over the course of fetal development. First, we applied the magnetic imaging technique of DTMRI, comparing the morphology of the midline commissures between 15 and 19 gestational weeks, during which the corpus callosum undergoes significant morphological change. At 15 gestational weeks, only the more rostral portion of the corpus callosum, made up of the rostrum, genu, and the body, can be seen (Fig. 1F), while the caudal portion of the corpus callosum, known as the splenium, does not become prominent until 18 to 19 gestational weeks (Fig. 1J and M; note the more caudal location of the red-colored callosal fibers). This

corroborates recent studies (using conventional MRI) suggesting that parts of the corpus callosum body directly over the fornix and the hippocampal commissure (visible in Fig. 1F) develop first, followed by the development of the splenium (Kier and Truwit, 1996, 1997). In contrast, the relative size of the anterior commissure appears unchanged between 15 (Fig. 1H) and 19 (Fig. 1N) gestational weeks. Previously, DTMRI has been successfully utilized to analyze the macro- and microstructural development of cerebral white matter tracts in living infants (Hüppi et al., 1998), and, in conjunction with fMRI, to trace the trajectories of major commissural and thalamocortical projections in the living adult human brain (Conturo et al., 1999). Our results indicate that DTMRI can be applied with equal success to the analysis of fixed embryonic tissue as well.

However, while DTMRI has shown itself to be a powerful and versatile technique, it is nonetheless an indirect visualization of fiber tracts in the brain, since it measures the anisotropic nature of water diffusion inside myelinated axon fibers, and not the fibers themselves. Therefore, data gathered via DTMRI must be verified using conventional histological methods that directly visualize axon tracts in the brain. To do this, we performed immunohistochemistry using the specific axonal markers neurofilament and GAP43. The results of the GAP43 immunostaining on sections from a 17-gestational-week brain are shown in Figure 2, where it is apparent that several major commissures have been clearly labeled by the GAP43 an-

tibody, and comparisons between coronal DTMRI slices and those sections that were immunostained demonstrate the accuracy of this novel imaging technique. A particular example can be seen by comparing Figure 1I (18 gestational weeks) and Figure 2C (17 gestational weeks); note the nearly identical morphology of the corpus callosum, the hippocampal commissure, and the internal capsule in two images generated via completely different techniques. While the spatial resolution of DTMRI remains too low to discern individual growth cones, it nonetheless represents a wholly noninvasive means of whole fiber tract visualization. Once the presence of an axonal structure has been verified using immunohistochemistry in one plane, DTMRI has the distinct advantage of allowing further analysis along the remaining planes, so that the true shape of a commissure can be defined. For instance, the three-dimensional shape of the hippocampal commissure and its angle and location in relationship to the corpus callosum in an 18-gestational-week human fetal brain can be appreciated with a glance in Figure 1I–K, while a conventional histological approach using coronal sections would only generate a series of small cross-sectional views of the same structure. Therefore, these data highlight the utility of the diffusion tensor imaging as an advanced emerging technique for analyzing multiple developing fiber tracts in the central nervous system, and in combination with immunostained sections from the same brain, it allows the most accurate interpretation of axonal tract morphology in the brain.

Presence of Midline Structures and Expression of Guidance Molecules in Human Fetal Brain

In the human brain, immunostaining experiments with subcallosal sling markers, NeuN, Nfia, and calretinin, demonstrated that midline populations analogous to the subcallosal sling are also present in the human fetal brain. At 13 gestational weeks, no sling development is apparent in the human. By week 15 of the gestation, a cluster of NeuN-positive cells appeared bilaterally at the lateral aspect of the corticoseptal boundary (arrow in Fig. 4F) and formed a recognizable sling by week 17 of gestation (arrow in Fig. 4L; labeled with calretinin). However, just like the glial wedge, the human subcallosal sling is not wholly identical to that observed in mouse. Immunostaining with the third sling marker, Nfia, reveals a second population of cells located dorsal to the corpus callosum at 15 gestational weeks (Fig. 4H and I), and it is not clear whether this is part of the human subcallosal sling or whether NeuN is also labeling some other distinctive cellular population (perhaps of cingulate or indusium griseum origin, based on the dorsal location) in the human fetal brain.

A second set of important midline structures consists of two midline glial populations, the glial wedge and the indusium griseum glia, situated below and above the corpus callosum, respectively (Shu and Richards, 2001). The GW and IGG guide callosal fibers by their secretion of the chemorepellant molecule *Slit2*. Both the GW and the IGG express the glial marker GFAP, but only the GW forms part of the radial glial scaffold (Howard et al., 2006) and labels with markers such as RC2, BLBP, and GLAST (Shu et al., 2003a). In humans, immunostaining using GFAP antibody revealed bilateral structures on both sides of the corpus callosum corresponding to the GW and the IGG (Fig. 3), which confirms the findings of Lent et al. (2005),

who also identified the presence of these structures in the human embryonic brain, and those of Rezaie et al. (2003), who analyzed GFAP staining in human fetuses between 19 and 23 weeks. In addition, Northern blot analysis demonstrates that both *Slit2*, which is secreted by the GW and IGG, and its axonal receptor *Robo1* are expressed in the fetal brain at 17 gestational weeks (Fig. 6). Although Northern blot analysis cannot show where these genes are being expressed, the relative intensity of expression levels between the dorsal and ventral telencephalon does fit the pattern expected from studies in mouse. *Robo1* and *Robo2*, which are expressed by the callosally projecting cortical neurons, are strongly expressed in the cortex. However, *Slit2*, which is expressed by the midline glia in mice, located at the corticoseptal boundary, shows stronger expression in the ventral forebrain (lane 3) compared to cortex (lane 1). The GFAP staining revealed apparent glial cell migration and demonstrated a dynamic pattern of glial differentiation during human fetal development. Interestingly, by 17 gestational weeks, GFAP-positive cells appear at the midline (Fig. 3L), and by 19 gestational weeks (Fig. 3N), the GFAP-positive glia are present within the human subcallosal sling (arrows), unlike the mouse, where very few GFAP-positive cells are ever found. In contrast, GFAP-positive glia are observed in the sling region in the developing cat brain at least during early callosal development (Silver et al., 1993) in a manner similar to what is observed here in humans, so it appears the distribution of GFAP-positive glia within the subcallosal sling varies across different mammalian species. It is unclear where these glia originate, but two possibilities are that they either originate from one of the midline glial populations (the GW, IGG, or MZG) or migrate to the midline from the cortical subventricular zone as sling neurons apparently do. One possible means to determine the origins of these cells is to perform *in situ* hybridization utilizing probes for *Slit2*, the guidance molecule only expressed by glial wedge cells. If these cells are in fact part of the glial wedge, then it would pose some interesting questions about this incongruity between mice and human brains and whether the greater size of the human embryonic brain requires *Slit2* secreting glial cells across the midline to prevent callosal fibers from entering the septum.

A third mechanism thought to play a role in callosal formation involves the initial axons that cross the midline and are known as the pioneering axons. In mouse, these fibers originate from the cingulate cortex and begin to cross the midline at E15.5 (Rash and Richards, 2001). These fibers are located in the dorsal region of the corpus callosum and project homotopically to the contralateral cingulate cortex. In mouse, neurons in the cingulate cortex also receive inputs from, and send projections to, the medial septum and diagonal band of Broca (MSDB) (Shu et al., 2001); this is known as the perforating pathway, since its fibers project across and perforate the developing corpus callosum. The pioneering axons are hypothesized to guide later crossing callosal fibers across the midline, and together they form large fasciculated bundles by E17. More recently, *Npn1*, a class 3 semaphorin receptor, was found to be expressed on these pioneering axons (Martins et al., 2004; Plachez et al., 2004). In humans, immunostaining with *Npn1* revealed heavily stained axonal structures within the corpus callosum at 17 weeks of gestation, demonstrating the presence of the cingulate pioneering

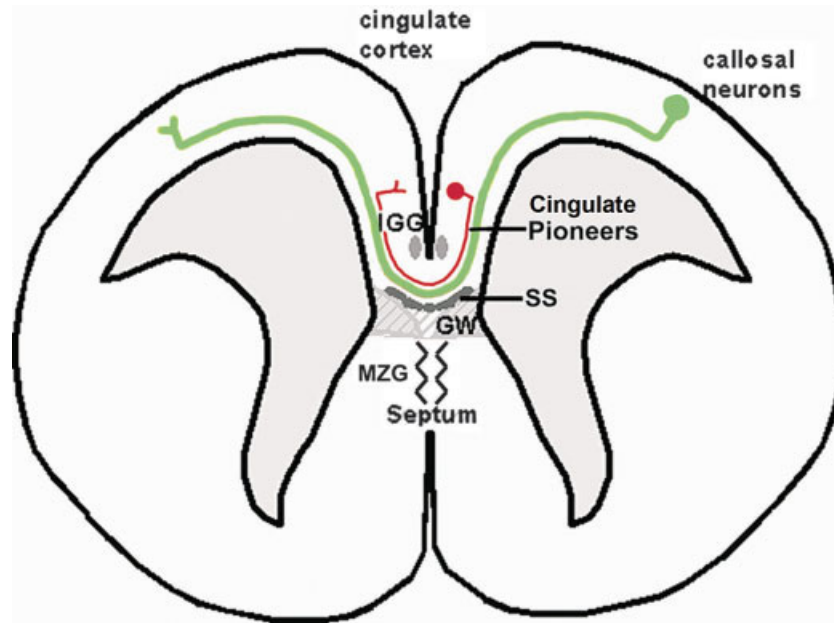


Fig. 7. Model of callosal development in the mouse. Schematic representation of key cellular and axonal populations along the midline that act in concert to mediate proper callosal axon (shown in green) pathfinding, including the glial wedge (GW), the indusium griseum glia (IGG), the subcallosal sling (SS), and cingulate pioneering axons (shown in red). MZG, midline zipper glia.

axons in humans. High-powered views of the labeled areas revealed numerous projections emerging from the cingulate cortex and projecting homotopically to the contralateral cingulate cortex (Fig. 5C). A prior study by deAzevedo et al. (1997) showed, via carbocyanine dye tract tracing, that the cingulate cortex contains callosally projecting neurons at 25–32 gestational weeks. By analyzing human brains from an earlier stage of embryonic development, we have shown the presence of cingulate-derived callosal fibers by 17 gestational weeks.

Together, the subcallosal sling, the midline glial populations, and the pioneering axons work in unison to guide axons across the midline in our mouse model of callosal formation (Fig. 7), and in this report, we present histological evidence that all three sets of structures are also present in the human. These histological data, coupled with the expression analysis of key commissural structural, guidance, and regulatory genes by Northern blot analysis, strongly support the notion that callosal fibers require multiple guidance mechanisms at both molecular and cellular level in order to cross the midline properly into the contralateral hemisphere, and that these same mechanisms are evolutionarily conserved.

Toward a Greater Understanding of Human Commissural Development

Interneuronal connectivity is the major underlying factor mediating both brain function and development. The complex system of axonal guidance mechanisms that govern the development of the major fiber tracts, including the forebrain commissures, plays a vital role in establishing this interconnectivity between the various regions of the growing embryonic brain. Recent studies by Bystron et al. (2005) in early human embryonic tissue demonstrate

the formation of nascent cellular and axonal networks beginning as early as the fourth week following conception, and prior to synaptogenesis, which may form the framework that guides future neuronal migration and axonal tract formation, further highlighting the importance of guidance mechanisms in the developing brain. If these mechanisms are disrupted, ACC and other commissural deformations can occur and often lead to devastating neurological and cognitive deficits. The various human congenital syndromes exhibiting ACC represent a wide genetic spectrum, including autosomal dominant disorders such as Apert syndrome and type 1 lissencephaly, autosomal recessive disorders such as Andermann syndrome, and X-linked disorders such as Aicardi syndrome. The overall phenotype and the clinical sequelae of commissural malformation disorders are equally heterogeneous. In addition to complete ACC, partial agenesis or hypoplastic formation of the corpus callosum can also be observed, and many other morphological or physiological defects, such as aniridia, micro- or macrocephaly, metabolic imbalance, and varying levels of physical or psychomotor retardation, can accompany the callosal defect. In order to better comprehend, diagnose, and hopefully prevent or treat these congenital disorders, we must fully understand how the corpus callosum develops normally. To date, significant progress has been made in constructing a model for callosal development in the mouse, in which a number of guidance molecules and cellular structures act in concert to guide commissural axons across the midline. Furthermore, targeted knockouts of genes involved in this model, such as *Slit2*, *Npn1*, *DCC*, *Netrin1*, *Nfia*, *Emx-1*, and *GAP43*, have generated multiple mouse models of callosal dysgenesis. This work has set the stage

for the study of normal and pathological commissural development in the human brain.

In this study, we confirm the presence of all key mouse midline structures and the expression of genes identified in mice that mediate midline axonal guidance in the developing human fetal brain. These results not only demonstrate that the mouse is an excellent model for studying callosal development in humans, but also serves as an excellent foundation for further studies utilizing human tissue. Now that some of the key structures have been defined morphologically, we can begin to assess the functional aspects of these structures; for instance, using *in situ* hybridization to examine the location of expression of candidate molecules. In addition, just as in mouse studies, the baseline knowledge of the elements of normal human callosal development allows for meaningful analysis of tissue from human brains affected by ACC. Finally, we introduce the use of DTMRI to define spatially multiple commissures in the developing human fetal brain, which has proven to be a powerful complement to the conventional histological approach to neuroanatomy.

ACKNOWLEDGMENTS

The authors gratefully acknowledge the work of the Maryland Brain and Tissue Bank for Developmental Disorders for providing the tissue used in these experiments, as well as the laboratory of Dr. D. Ginty (Johns Hopkins University School of Medicine) for providing the Npn1 antibody.

LITERATURE CITED

- Bagri A, Marin O, Plump AS, Mak J, Pleasure SJ, Rubenstein JL, Tessier-Lavigne M. 2002. Slit proteins prevent midline crossing and determine the dorsoventral position of major axonal pathways in the mammalian forebrain. *Neuron* 33:153–155.
- Bagnard D, Lohrum M, Uziel D, Puschel AW, Bolz J. 1998. Semaphorins act as attractive and repulsive guidance signals during the development of cortical projections. *Development* 125:5043–5053.
- Basser PJ, Mattiello J, Le Bihan D. 1994. MR diffusion tensor spectroscopy and imaging. *Biophys J* 66:259–267.
- Bystron I, Molnar Z, Otellin V, Blakemore C. 2005. Tangential networks of precocious neurons and early axonal outgrowth in the embryonic human forebrain. *J Neurosci* 25:2781–2792.
- Conturo TE, Lori NF, Cull TS, Akbudak E, Snyder AZ, Shimony JS, McKinstry RC, Burton H, Raichle ME. 1999. Tracking neuronal fiber pathways in the living human brain. *Proc Natl Acad Sci USA* 96:10422–10427.
- Cummings DM, Malun D, Brunjes PC. 1997. Development of the anterior commissure in the opossum: midline extracellular space and glia coincide with early axon decussation. *J Neurobiol* 32:403–414.
- deAzevedo LC, Hedin-Pereira C, Lent R. 1997. Callosal neurons in the cingulate cortical plate and subplate of human fetuses. *J Comp Neurol* 386:60–70.
- Edsjo A, Nilsson H, Vandesompele J, Karlsson J, Pattyn F, Culp LA, Speleman F, Pahlman S. 2004. Neuroblastoma cells with overexpressed MYCN retain their capacity to undergo neuronal differentiation. *Lab Invest* 84:406–417.
- Ellezam B, Selles-Navarro I, Manitt C, Kennedy TE, McKerracher L. 2001. Expression of netrin-1 and its receptors DCC and UNC-5H2 after axotomy and during regeneration of adult rat retinal ganglion cells. *Exp Neurol* 168:105–115.
- Fazeli A, Dickinson SL, Hermiston ML, Tighe RV, Steen RG, Small CG, Stoeckli ET, Keino-Masu K, Masu M, Rayburn H, Simons J, Bronson RT, Gordon JI, Tessier-Lavigne M, Weinberg RA. 1997. Phenotype of mice lacking functional deleted in colorectal cancer (DCC) gene. *Nature* 386:796–804.
- Gu C, Rodriguez ER, Reimert DV, Shu T, Fritsch B, Richards LJ, Kolodkin AL, Ginty DD. 2003. Nueropilin-1 conveys semaphoring and VEGF signaling during neural and cardiovascular development. *Dev Cell* 5:45–57.
- Hewitt W. 1962. The development of the human corpus callosum. *J Anat* 96:355–358.
- Howard B, Chen Y, Zecevic N. 2006. Cortical progenitor cells in the developing human telencephalon. *Glia* 53:57–66.
- Hüppi PS, Maier SE, Peled S, Zientara GP, Barnes PD, Jolesz FA, Volpe JJ. 1998. Microstructural development of human newborn cerebral white matter assessed *in vivo* by diffusion tensor magnetic resonance imaging. *Pediatr Res* 44:584–590.
- Itoh A, Miyabayashi T, Ohno M, Sakano S. 1998. Cloning and expressions of three mammalian homologues of *Drosophila* slit suggest possible roles for Slit in the formation and maintenance of the nervous system. *Brain Res Mol Brain Res* 62:175–186.
- Jeret JS, Serur D, Wisniewski KE, Lubin RA. 1987. Clinicopathological findings associated with agenesis of the corpus callosum. *Brain Dev* 9:255–264.
- Kier EL, Truwit CL. 1996. The normal and abnormal genu of the corpus callosum: an evolutionary, embryologic, anatomic and MR analysis. *Am J Neurol Res* 17:1631–1641.
- Kier EL, Truwit CL. 1997. The lamina rostralis: modification of concepts concerning the anatomy, embryology, and MR appearance of the rostrum of the corpus callosum. *Am J Neurol Res* 18:715–722.
- Koester SE, O'Leary DD. 1994. Axons of early generated neurons in cingulate cortex pioneer the corpus callosum. *J Neurosci* 14:6608–6620.
- Lent R, Uziel D, Baudrimont M, Fallet C. 2005. Cellular and molecular tunnels surrounding the forebrain commissures of human fetuses. *J Comp Neurol* 483:375–382.
- Marcus RC, Blazeski R, Godement P, Mason CA. 1995. Retinal axon divergence in the optic chiasm: uncrossed axons diverge from crossed axons within a midline glial specialization. *J Neurosci* 15:3716–3729.
- Martins GJ, Plachez C, Richards LJ. 2004. Cingulate pioneering axons are required for development of the rostral corpus callosum. San Diego: Society for Neuroscience 34th Annual Meeting.
- Meyerhardt JA, Look AT, Bigner SH, Fearon ER. 1997. Identification and characterization of neogenin, a DCC-related gene. *Oncogene* 14:1129–1136.
- Misawa H, Yamaguchi M. 2002. Identification of transcription factor in the promoter region of rat regucalcin gene: binding of nuclear factor I-A1 to TTGGC motif. *J Cell Biochem* 84:795–802.
- Mori S, van Zijl PC. 1998. A motion correction scheme by twin-echo navigation for diffusion-weighted magnetic resonance imaging with multiple RF echo acquisition. *Magn Reson Med* 40:511–516.
- Morita T, Nitta H, Kiyama Y, Mori H, Mishina M. 1995. Differential expression of two zebrafish *emx* homeoprotein mRNAs in the developing brain. *Neurosci Lett* 198:131–134.
- Norman MG, McGillivray BC, Kalousek DK, Hill A, Poskitt KJ. 1995. Crossing the midline. In: Becker LE, Cochrane DD, Muenke M, editors. *Congenital malformations of the brain: pathological, embryological, clinical, radiological and genetic aspects*. New York: Oxford University Press. p 309–331.
- Ozaki HS, Wahlsten D. 1992. Prenatal formation of the normal mouse corpus callosum: a quantitative study with carbocyanine dyes. *J Comp Neurol* 323:81–90.
- Pellegrini M, Mansouri A, Simeone A, Boncinelli E, Gruss P. 1996. Dentate gyrus formation requires *Emx2*. *Development* 122:3893–3898.
- Pierpaoli C, Basser PJ. 1996. Toward a quantitative assessment of diffusion anisotropy. *Magn Reson Med* 36:893–906.
- Plachez C, Gu C, Richards LJ. 2004. Aberrant projection of callosal pioneering axons in Npn1 Sema mice. San Diego, CA: Society for Neuroscience 34th Annual Meeting.
- Polleux F, Giger RJ, Ginty DD, Kolodkin AL, Ghosh A. 1998. Patterning of cortical efferent projections by semaphoring-neuropilin interactions. *Science* 282:1904–1906.
- Qiu M, Anderson S, Chen S, Meneses JJ, Hevner R, Kuwana E, Pedersen RA, Rubenstein JL. 1996. Mutation of the *Emx-1* homeobox gene disrupts the corpus callosum. *Dev Biol* 178:174–178.
- Rakic P, Yakovlev PI. 1968. Development of the corpus callosum and cavum septi in man. *J Comp Neurol* 132:45–72.

- Rash BG, Richards LJ. 2001. A role for cingulate pioneering axons in the development of the corpus callosum. *J Comp Neurol* 434:147–157.
- Rezaie P, Ulfing N, Male D. 2003. Distribution and morphology of GFAP-positive astrocytes in the human fetal brain at second trimester. *Neuroembryology* 2:50–63.
- Richards LJ. 2002. Axonal pathfinding mechanisms at the cortical midline and in the development of the corpus callosum. *Braz J Med Biol Res* 35:1431–1439.
- Richards LJ, Andrews WD, Zhang J, Mori S, Sundaresan V, Plachez C. 2004a. Robo1 and Robo2 knockout mice display commissural defects in the brain. San Diego, CA: Society for Neuroscience 34th Annual Meeting.
- Richards LJ, Plachez C, Ren T. 2004b. Mechanisms regulating the development of the corpus callosum and its agenesis in mouse and human. *Clin Genet* 66:276–289.
- Serafini T, Colamarino SA, Leonardo ED, Wang H, Beddington R, Skarnes WC, Tessier-Lavigne M. 1996. Netrin-1 is required for commissural axon guidance in the developing vertebrate nervous system. *Cell* 87:1001–1014.
- Shen Y, Mani S, Donovan SL, Schowb JE, Meiri KF. 2002. Growth-associated protein-43 is required for commissural axon guidance in the developing vertebrate nervous system. *J Neurosci* 22:239–247.
- Shu T, Richards LJ. 2001. Cortical axon guidance by the glial wedge during development of the corpus callosum. *J Neurosci* 21:2749–2758.
- Shu T, Shen WB, Richards LJ. 2001. Development of the perforating pathway: an ipsilaterally projecting pathway between the medial septum/diagonal band of Broca and the cingulate cortex that intersects the corpus callosum. *J Comp Neurol* 436:411–422.
- Shu T, Puche AC, Richards LJ. 2003a. Development of midline glial populations at the corticoseptal boundary. *J Neurobiol* 57:81–94.
- Shu T, Butz KG, Plachez C, Gronostajski RM, Richards LJ. 2003b. Abnormal development of forebrain midline glia and commissural projections in Nfia knock-out mice. *J Neurosci* 23:203–212.
- Shu T, Li Y, Keller A, Richards LJ. 2003c. The glial sling is a migratory population of developing neurons. *Development* 130:2929–2937.
- Silver J, Lorenz SE, Wahlsten D, Coughlin J. 1982. Axonal guidance during development of the great cerebral commissures: descriptive and experimental studies, in vivo, on the role of preformed glial pathways. *J Comp Neurol* 210:10–29.
- Silver J, Ogawa MY. 1983. Postnatally induced formation of the corpus callosum in acallosal mice on glia-coated cellulose bridges. *Science* 220:1067–1069.
- Silver J, Edwards MA, Levitt P. 1993. Immunocytochemical demonstrations of early appearing astroglial structures that form boundaries and pathways along axon tracts in the fetal brain. *J Comp Neurol* 328:415–436.
- Sundaresan V, Mambetisaeva E, Andrews W, Annan A, Knoll B, Tear G, Bannister L. 2004. Dynamic expression patterns of Robo (Robo1 and Robo2) in the developing murine central nervous system. *J Comp Neurol* 468:467–481.
- Wang LC, Dani J, Godement P, Marcus RC, Mason CA. 1995. Crossed and uncrossed retinal axons respond differently to cells of the optic chiasm midline in vitro. *Neuron* 15:1349–1364.
- Watson RE, Wiegand SJ, Clough RW, Hoffman GE. 1986. Use of cryoprotectant to maintain long-term peptide immunoreactivity and tissue morphology. *Peptides* 7:155–159.
- Wisniewski KE, Jeret JS. 1991. Callosal agenesis: review of pathological and cytogenetic features, in clinical description and related disorders. In: Lassonde M, Jeeves MA, editors. *Callosal agenesis: a natural split brain*. New York: Plenum Press. p 1–6.
- Yoshida M, Suda Y, Matsuo I, Miyamoto N, Takeda N, Kuratani S, Aizawa S. 1997. Emx1 and Emx2 functions in development of dorsal telencephalon. *Development* 124:101–111.